Scripta Materialia 142 (2018) 41–45

Contents lists available at ScienceDirect

Scripta Materialia

journal homepage: www.elsevier.com/locate/scriptamat

Regular article

Precipitation of α′ in neutron irradiated commercial FeCrAl alloys☆

Kevin G. Field [a,*], Kenneth C. Littrell [a], Samuel A. Briggs [b]

[a] Oak Ridge National Laboratory, Oak Ridge, TN 37831, USA
[b] University of Wisconsin, Madison, WI 53706, USA

ARTICLE INFO

Article history:
Received 27 March 2017
Received in revised form 3 July 2017
Accepted 14 August 2017
Available online xxxx

Keywords:
FeCrAl
Neutron diffraction
Precipitation
Ferritic steels

ABSTRACT

Alkrothal 720 and Kanthal APMT™, two commercial FeCrAl alloys, were neutron irradiated up to damage doses of 7.0 displacements per atom (dpa) in the temperature range of 320 to 382 °C to characterize the α′ precipitation in these alloys using small-angle neutron scattering. Both alloys exhibited α′ precipitation. Kanthal APMT™ exhibited higher number densities and volume fraction, a result attributed to its higher Cr content compared with Alkrothal 720. Trends observed as a function of damage dose (dpa) are consistent with literature trends for both FeCr and FeCrAl alloys.

High chromium (Cr) ferritic/martensitic steels are frequently investigated for applications requiring elevated temperatures and oxidation and/or corrosion resistance. The elevated Cr content (typically >7–8 at.%) enables acceptable oxidation and corrosion resistance in a range of elevated-temperature environments such as air, water, and steam. Many of these ferritic steel alloys are susceptible to embrittlement at service temperatures of ~500 °C or below. This embrittlement phenomenon is classically referred to as "475 °C embrittlement," and decades of research have been dedicated to understanding its cause. It is now accepted that the embrittlement results from a miscibility gap below 500 °C in the Fe-Cr phase diagram, where precipitation of the Cr-rich α′ phase occurs through either a nucleation and growth process or spinodal decomposition in the Fe-rich α matrix when the Cr content of the alloy exceeds ~8.5 at.% [1,2].

Detailed studies of the Fe-Cr system show that the mechanism, rate, and magnitude of the precipitation of the α′ phase depend on both the service temperature and composition of the ferritic-based stainless steel [3]. For example, Grobner [4] and Courtnall and Pickering [5] summarize the effects of alloying and show most practical alloying elements, such as Ti, Mo, and Nb, lead to an increased rate in hardening linked to α′ precipitation. Additional studies [2,6] show the detrimental effect of increased Cr content in FeCr alloys upon α′ precipitation and the resulting mechanical performance. It appears that traditional metallurgy practices have little effect on mitigating α′ embrittlement. However, renewed interest in FeCrAl-based alloys for applications below ~500 °C has triggered the rediscovery of the benefits of significant additions of aluminum (Al) (≥2.5 at.%) [7,8] on α′ precipitation. Although Al additions often provide a benefit in suppressing α′ precipitation, many industrial alloys—such as PM2000, MA956, and AISI Type 406—have proved to still be susceptible to α′ formation [9–14].

This study seeks to expand the current database of α′ precipitation in commercially available FeCrAl alloys to provide insight into their viability in industrial applications in which service temperatures reside below 500 °C. Specifically, the interest of this study is to examine candidate FeCrAl alloys for accident tolerant fuel (ATF) cladding applications where service temperatures are expected to be near 300 °C but off-normal conditions can exceed temperatures above 1000 °C [15]. Coupons of commercial alloys were neutron irradiated and then characterized using small-angle neutron scattering (SANS). Neutron irradiation has been shown to increase the rate of α′ precipitation [2,6,16–18] and hence accelerate the speed of detection of α′ and rapid progression to the growth-based regime for alloys where nucleation and growth is expected. SANS is widely used for characterization of α′ precipitation in both FeCr [13,18–21] and FeCrAl alloys [3,17,22,23], and our recent work shows good agreement can be achieved between SANS and more time-intensive atom probe tomography studies [17].

Two commercial FeCrAl alloys, Kanthal APMT™ and Alkrothal 720, were used for this study. Kanthal APMT™ is a 21.95 at.% Cr–9.64 at.% Al–1.52 at.% Mo, powder-metallurgy–derived FeCrAl alloy; the heat and hence composition is the same as in Ref. [24]. Alkrothal 720 is a 13.13 at.% Cr–8.22 at.% Al, wrought FeCrAl alloy; its composition and

* Corresponding author at: Materials Science and Technology Division, PO Box 2008, Oak Ridge, TN 37831, USA.
E-mail addresses: fieldkg@ornl.gov (K.G. Field), littrellkc@ornl.gov (K.C. Littrell), sbriggs@sandia.gov (S.A. Briggs).

http://dx.doi.org/10.1016/j.scriptamat.2017.08.022
1359-6462/

starting microstructure are found in Ref. [25]. Only two commercial alloys were studied due to the limited sample volume capacity of the neutron irradiation rig used. The selected alloys represent two uniquely different alloy types: one in which α′ precipitation is expected to occur in great magnitude (Kanthal APMT™) and one in which little or no α′ precipitation is expected (Alkrothal 720) but both alloys still exhibit high temperature (1200 °C) steam oxidation resistance, a key requirement for ATF cladding applications [26,27]. Additionally, the Mo additions in the Kanthal APMT™ alloy allow for possible insights into any additional effects due to minor alloying additions or powder metallurgy fabrication approach. Bulk Kanthal APMT™ was fabricated in rod form and bulk Alkrothal 720 specimens in thin sheet form.

Neutron irradiations were conducted in Oak Ridge National Laboratory's (ORNL's) High Flux Isotope Reactor (HFIR). Full details regarding the specimen configuration and irradiations are found in Refs. [16,17,23–25]; only a brief description is provided here. Kanthal APMT™ was neutron irradiated to 0.3, 1.8, and 7.0 displacement per atom (dpa) at temperatures of 334.5 ± 0.6 °C, 381.9 ± 5.4 °C, and 319.9 ± 12.7 °C, respectively. Alkrothal 720 was neutron irradiated to 0.8, 1.8, and 7.0 dpa at temperatures of 355.1 ± 3.4 °C, 381.9 ± 5.4 °C, and 319.9 ± 12.7 °C, respectively. The dose ranges represent the transient regime for the mechanical properties of FeCrAl alloys under irradiation conditions relevant toward early- to mid-life cladding conditions during light water reactor operation [24]. All irradiations were conducted with a neutron flux between 8.54×10^{14} and 8.84×10^{14} n/cm^2 s (E > 0.1 MeV), resulting in dose rates in the range of 7.7×10^{-7} to 8.1×10^{-7} dpa/s.

Tensile coupons of both the as-received and neutron-irradiated condition were tested in a shielded hot cell facility; data from these tests are presented elsewhere [24,28]. Following the tensile tests, one-half of each broken tensile specimen was prepared and shipped to the HFIR General Purpose SANS [29] beam line. The SANS detector configuration and data reduction techniques were identical to those described in Ref. [17].

Scattering intensities were modeled using a simplified approach in which α′ precipitates are considered monodispersed spheres within the α matrix and exhibit a hard-sphere potential. Additionally, an inherent background contribution was found owing to large impurities, precipitates, and grain boundaries in the alloys that result in an additional low-q inverse power law completed in summation [30]. No contribution of the reactive element-rich particles in the Kanthal APMT™ specimens in the q-range studied were observed due to their large particles sizes (100–500 nm) [31]. The result is that $I(q)$ takes the functional form of

$$I(q) = V\eta^{\alpha'}\Delta\rho^2 P(q,r)S(q,R_{hs},\eta) + (Aq^{-m} + B), \quad (1)$$

where V is the volume of the precipitates; $\eta^{\alpha'}$ is the volume fraction of α′ precipitates; $\Delta\rho$ is the scattering length density difference between the α′ phase and the α matrix; $P(q,r)$ is the particle form factor for spherical precipitates [32]; $S(q,R_{hs},\eta)$ is the hard-sphere structure factor [30]; and $Aq^{-m} + B$ is the inverse power law, where A is the power law length scale factor, m is the power law exponent, and B is the residual background in the measurements. This functional form was fitted to the experimental data using a modified Levenberg-Marquardt algorithm. Values of interest, including precipitate volume fraction, number density, and radius of the α′ precipitates, can be derived from the fitting parameters using the method described by Pedersen [30]. Using simplifying assumptions in the determined scattering contrast, as described in previous work [17], the composition of the α′ precipitates and the α matrix can be estimated by

$$C_{Cr}^{matrix} = \overline{C}_{Cr} - \frac{\eta^{\alpha'}\Delta\rho a_o^3}{4(b_{Fe} - b_{Cr})} \quad (2)$$

and

$$C_{Cr}^{\alpha'} = \left[\overline{C}_{Cr} - \left(1 - \eta^{\alpha'}\right)C_{Cr}^{matrix}\right]/\eta^{\alpha'}, \quad (3)$$

where $\overline{C}_{Cr}$ is the bulk composition of Cr in atomic fraction, C_{Cr}^{matrix} is the atomic fraction of Cr in the matrix, $C_{Cr}^{\alpha'}$ is the atomic fraction of Cr in the α′ precipitates, a_o is the lattice parameter (2.87 Å), and b_{Fe} and b_{Cr} are scattering lengths of Fe and Cr respectively. Reported errors for all values are based on the standard error of the fitting coefficients and any subsequent error propagation [30]. The assumed model has been applied to neutron-irradiated model FeCrAl alloys and shown good experimental matching for both morphology and composition values with atom probe tomography results at higher doses where a coarsening regime is expected [17].

Fig. 1 shows the scattering curves, including the best-fit determined model for both alloys. The unirradiated curves in Fig. 1 show only the low-Q inverse power law contribution to the scattering curves, indicating no significant Cr-clustering or α′ precipitation in these alloys before irradiation. After irradiation, a characteristic peak is observed in the SANS scattering curves stemming from the presence of α′ precipitates within the matrix. A clear change in this peak with increasing damage dose (dpa) is seen for both Kanthal APMT™ and Alkrothal 720. For both alloys, the peaks shift toward lower Q and the magnitude of the peaks increase with increasing damage dose (dpa). The relative change in this trend is more apparent in higher-Cr Kanthal APMT™ than in Alkrothal 720. Qualitatively, these trends suggest that with increasing dose, a lower number density of precipitates are present in both alloys; but a significantly higher volume fraction exists within the Kanthal APMT™ matrix, as expected.

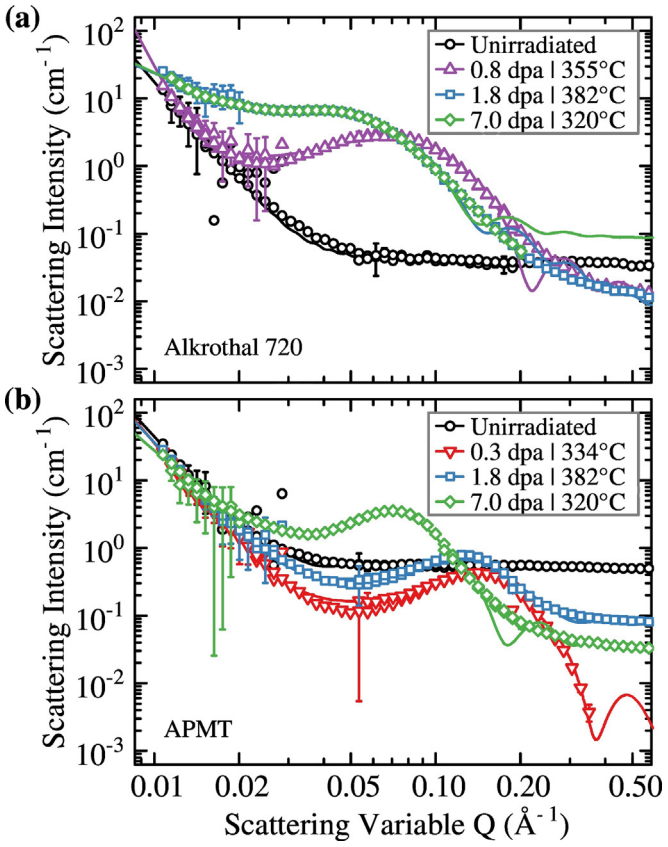

Fig. 1. Experimental scattering intensities (symbols) and best-fit model (lines) of neutron-irradiated commercial FeCrAl alloys: (a) Alkrothal 720 and (b) Kanthal APMT™.